Chinese Chemical Letters 35 (2024) 109090

Contents lists available at ScienceDirect

Chinese Chemical Letters

journal homepage: www.elsevier.com/locate/cclet

Tuning the membrane rejection behavior by surface wettability engineering for an effective water-in-oil emulsion separation

Yan Zou[a], Yin-Shuang Hu[b,c], Deng-Hui Tian[a], Hong Wu[a], Xiaoshu Lv[a], Guangming Jiang[a,*], Yu-Xi Huang[b,c,*]

[a] Engineering Research Center for Waste Oil Recovery Technology and Equipment, Ministry of Education, Chongqing Technology and Business University, Chongqing 400067, China
[b] School of Environmental Science and Engineering, Sun Yat-sen University, Guangzhou 510275, China
[c] Guangdong Provincial Key Laboratory of Environmental Pollution Control and Remediation Technology (Sun Yat-sen University), Guangzhou 510275, China

ARTICLE INFO

Article history:
Received 30 June 2023
Revised 8 September 2023
Accepted 12 September 2023
Available online 17 September 2023

Keywords:
Water-in-oil emulsion
Ceramic membrane
Membrane separation
Surface wettability

ABSTRACT

Membrane-based separation is a promising technology to eliminate water impurities from the oil phase. However, it remains a great challenge to separate water from highly emulsified viscous oil owing to the high stability of the water droplets in oil. Herein we report a surface wettability engineering on an alumina ceramic membrane to achieve an efficient separation of a water-in-oil (W/O) emulsion. Silanes with different carbon chain lengths and fluorinated status were introduced to endow the alumina membrane with different surface wettabilities. While all the modified membranes exhibited excellent separation of the W/O without Span 80 (surfactant), the one with amphiphobic wettability and lowest surface energy failed to separate the Span 80 stabilized W/O. The presence of Span 80 reduced the interfacial tension of water droplets, making them easier to deform and penetrate the modified membrane with the lowest surface energy. It reveals that engineering proper surface wettability is the key to separating the oil and water phases. Besides, the modified membranes maintained decent separation performance and stability under long-term run separation of the emulsified W/O.

The increasing waste oil discharge from anthropogenic activities such as petrochemical, food, textile, and mechanical industries has become a critical issue for the environment [1,2]. These waste oils have complex compositions and are harmful to the ecological system [3,4], and have been listed as hazardous solid waste by the Ministry of Ecology and Environmental Protection of China. Oil recycling offers a sustainable venue for treating these waste oils [5]. However, one major challenge is that the waste oil is usually highly emulsified with water and surfactant (classified as the water-in-oil emulsion, W/O), which makes it extremely difficult to be purified [6]. Therefore, the separation of oil and water emulsion has become an emerging issue in both academic and industrial communities.

Compared with traditional techniques such as mechanical and absorption separation [7], membrane separation has emerged as a competitive candidate for emulsified oil separation owing to its high efficiency, low chemical consumption, and continuous operation mode [8,9]. Numerous efforts have been dedicated to the design of membrane materials with special wettabilities, most of which focused on superhydrophilic membranes for treating oil-in-water emulsions (O/W) [10,11]. It is obvious that the membrane wettability for separating W/O is quite different from what is needed for O/W. In fact, the separation of W/O emulsion is more challenging than the O/W because of the much higher viscosity and the lower density of the oil phase compared to the water phase. Such features make the W/O emulsion separation process kinetically slow and hard to take advantage of gravity as the driving force.

It is widely accepted that the membrane surface should be hydrophobic and oleophilic for W/O emulsion separation so that the membrane can repel the water droplets while allowing the oil to transfer. Based on this consideration, researchers have employed low surface energy materials like fluorinated alkyl silane (FAS) [12], polytetrafluoroethylene (PTFE) [13,14], and polydimethylsiloxane (PDMS) [15] to construct a superhydrophobic/superoleophilic surface [16,17]. Li *et al.* prepared a superhydrophobic fiberglass membrane, which shows high separation efficiency above 99% for water-in-liquid paraffin emulsions [18]. Zhang *et al.* reported a copper oxide-based superhydrophobic microfiltration membrane,

* Corresponding authors.
E-mail addresses: jiangguangming@zju.edu.cn (G. Jiang), huangyx253@mail.sysu.edu.cn (Y.-X. Huang).

https://doi.org/10.1016/j.cclet.2023.109090
1001-8417/

which was used for separating various water-in-transformer oil emulsions with an efficiency exceeding 99.995% [19]. However, most of researches used low-viscous organic solvents, such as toluene and hexane, to prepare the synthetic W/O emulsion (Table S1 in Supporting information). It remains unknown how the membrane surface wettability impacts the W/O emulsion separation when the oil phase is relatively viscous, let alone the correlation between wettability and separation efficacy. Moreover, the long-term stability and performance of the membranes also need to be investigated for practical application purposes.

Herein the commercial alumina membrane was employed as the substrate, the surface energy of which was further engineered *via* surface silane modifications to construct oleophilic membranes for separating water-in-transformer oil emulsion. Four silanes with different carbon chain lengths and fluorinated statuses were introduced to evaluate the carbon chain and fluorination effects on the surface wettability. The separation performance and the membrane stability of the as-prepared membranes were then investigated towards the W/O emulsions with and without the presence of Span 80. Finally, the W/O emulsion separation mechanism with different types of silanes was discussed.

The commercial alumina membrane has an α-Al_2O_3 phase, as proved by the XRD result (Fig. S2 in Supporting information). Since alumina is a hydrophilic material, it is necessary to reverse its wettability to oleophilic for the W/O emulsion separation. Based on this consideration, four different silanes were chosen to endow the membrane with oleophilicity, *i.e.*, C_3, C_3-F, C_{10}, and C_{10}-F. The four silanes were distinguished by the carbon chain length and fluorinated status. The modified alumina membranes are denoted as C_3/M, C_3-F/M, C_{10}/M, and C_{10}-F/M, respectively (detailed experimental section is given in Supporting information). All five membranes showed similar dense porous structures, suggesting the silane modification did not significantly affect the membrane structure (Figs. 1a-e). Surface elemental analyses using SEM-EDS demonstrated that the silane-modified membranes exhibited much stronger C and Si signals than the pristine alumina membrane. Besides, the F signals on the C_3-F/M and C_{10}-F/M were stronger than those on the other three, indicating the successful modification of fluorinated silanes.

The surface chemical compositions of the above membranes were further analyzed by XPS. After silane modifications, the surface elemental compositions of the membranes exhibited significant changes (Table S2 in Supporting information). The increase of the relative amounts of C and Si for all the modified membranes demonstrated the occupation of the silanes on the surface. The surface atomic ratios of F were 27.3% and 28.54% for the C_3-F/M and C_{10}-F/M membranes, respectively, further confirming the presence of fluorinated silanes. These results also indicate the high modification densities of those silanes on the alumina surface. In addition, the high-resolution XPS spectra of C 1s clearly revealed the presence of -CH_2–CF_3 and -CH_2–CF_2- for the C_3-F and C_{10}-F/M membranes, respectively (Fig. 1f) [20]. In the F 1s spectra, only one peak was observed for the C_3-F/M membranes representing the terminal group -CF_3. For the C_{10}-F/M membrane, two peaks could be detected representing -CF_2- and -CF_3, respectively (Fig. 1g). Besides, the Si-O bonding was also significant in the XPS spectra, which was formed during the silane hydrolysis process. Moreover, both C_3/M and C_3-F/M membranes showed higher peak intensity than C_{10}/M and C_{10}-F/M membranes (Fig. 1h), indicating that silanes with short carbon chains hydrolyzed more easily than those with long carbon chains.

The surface wettability of the as-prepared membranes was evaluated by the contact angles (CAs) tests. As observed in Fig. 2a, the original pristine alumina membrane could be instantly wetted by water, mineral oil, and transformer oil droplets. On the other hand, Span 80 did not completely wet the pristine membrane, although its CA was relatively low ($< 20°$). This observation could be ascribed to the highly viscous nature of the Span 80 and its relatively low hydrophilic-lipophilic balance (HLB) value (4.3), which prevented it from fully spreading over the hydrophilic alumina surface. In comparison, distinct CA changes were observed after silane modification. The C_{10}-F/M exhibited the highest CAs for all four testing liquids, which was obviously due to the fluorinated long carbon chain silane modification that endowed the membrane with low surface energy [21,22]. In contrast, the C_{10}/M showed a high CA for water but low CAs for Span 80 and mineral oil. This result is expected because the C_{10} silane is hydrophobic and oleophilic. Besides, due to its lower viscosity than mineral oil, the transformer oil droplet could completely wet into the C_{10}/M membrane.

Counterintuitive results were observed for the CA measurements on the short-chain silane-modified membranes. The water CA on the C_3/M membrane was about 142°, much higher than that on the C_3-F/M membrane and even the C_{10}/M membrane. This observation should be associated with the silane hydrolysis process, which was also indicated by the XPS results (Fig. 1h). We have recently demonstrated that small silica nanoparticles (NPs) will be formed during the hydrolysis process when using triple hydrolysis site silanes [23]. In this study, all four silanes have triple hydrolysis sites, and thus theoretically, they would all crosslink into silica nanoparticles during surface modification. However, silanes with a longer carbon chain would be more difficult to crosslink than shorter ones due to the greater steric hindrance. Similarly, fluorinated silanes would be even harder to crosslink due to the lower surface energy (Fig. 2b). Based on the above considerations, it is very likely that the C_3 silane would generate more SiO_2 NPs on the surface than its fluorinated counterpart, resulting in higher surface roughness. According to the Cassie-Baxter theory, a higher roughness would lead to a higher apparent CA [24]. Therefore, the water CA on the C_3/M membrane was higher than the C_3-F/M and even the C_{10}/M membrane. On the other hand, while the transformer oil droplet wetted the C_3/M membrane, the Span 80 and mineral oil had much smaller CAs on the C_3/M membrane compared to those on the C_3-F/M membrane. These results could be explained by the Wenzel theory, which can be applied when the rough surface is in complete contact with the testing liquid. In these scenarios, the Wenzel theory predicts that a higher roughness will result in a smaller apparent CA, which is in good agreement with our observations [24].

Liquid entry pressure measurement was conducted to identify suitable operation pressures for the five membranes. According to the classical theory, the LEP can be calculated by the following equation (Eq. 1) [25,26]:

$$\mathrm{LEP} = -\frac{2B\gamma_1 \cos\theta_0}{r} \tag{1}$$

where B is a geometric factor accounting for the noncylindrical nature of the membrane pore structure, γ_1 is the liquid surface tension, θ_0 is the intrinsic contact angle, and r is the equivalent pore radius. Assuming that the pore size and pore geometry did not change after silane modification, the LEP will be mainly determined by the CA of the liquid. The LEP results shown in Fig. 2c met the above assumption quite well. The four modified membranes showed oleophilic properties as their transformer oil LEPs were lower than their water LEPs, opposite to the pristine membrane. It is also worth noting that the water LEP of the C_3/M membrane was higher than that of the C_3-F/M membrane, consistent with Eq. 1 and water CA results. In the case of the C_{10}-F/M membrane, CA measurements revealed that it is actually amphiphobic. Consequently, it is more difficult for the oil phase to permeate through the C_{10}-F/M membrane, which is why its oil LEP is higher than other modified membranes. Nevertheless, its oil LEP

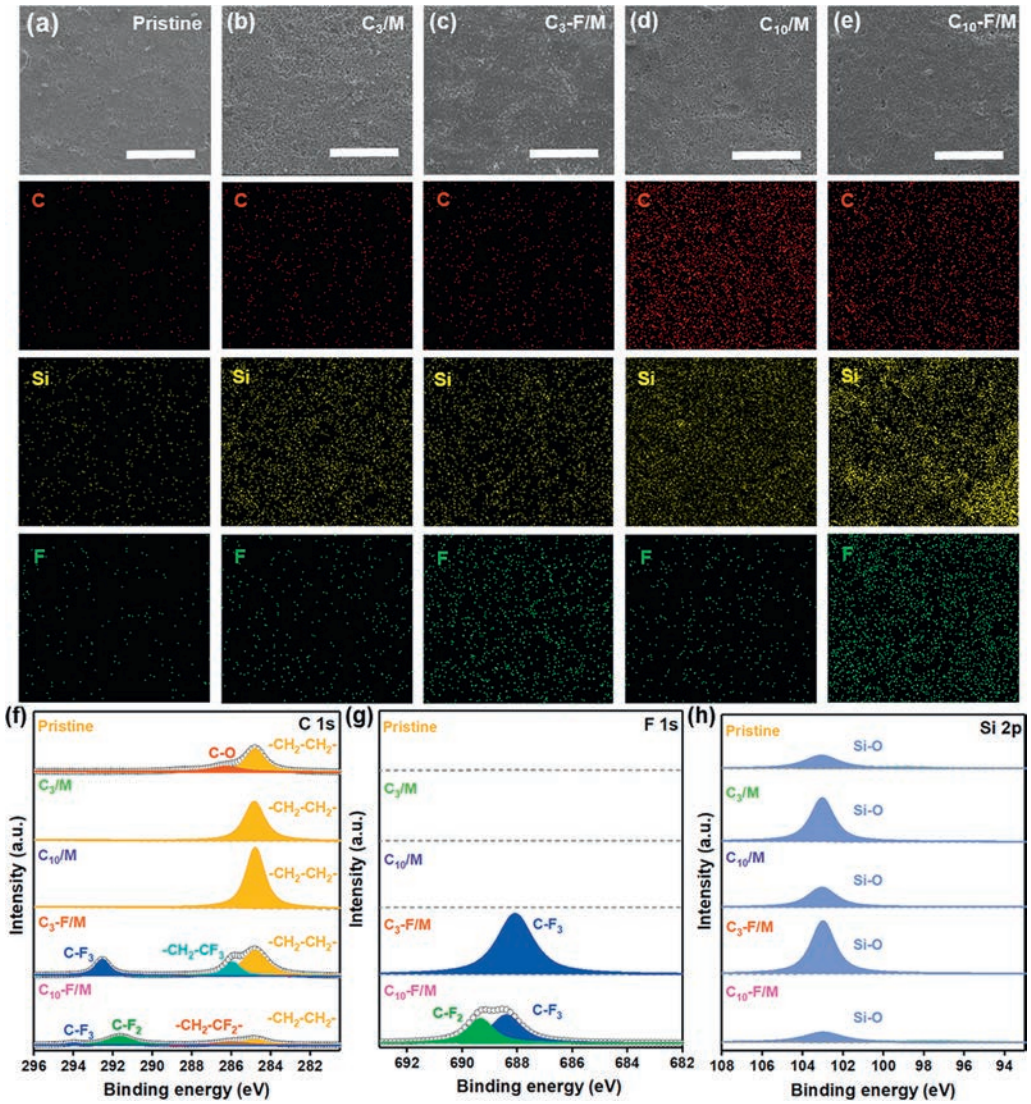

Fig. 1. SEM images and the corresponding elemental mappings of the pristine alumina (a), C_3/M (b), C_3-F/M (c), C_{10}/M (d), and C_{10}-F/M (e) membranes. The scale bar represents 100 μm. And the XPS spectra of the as-prepared membranes: (f) C 1s, (g) F 1s, and (h) Si 2p.

was lower than the water, suggesting that the C_{10}-F/M membrane was still suitable for the separation of W/O emulsion.

Unlike the separation of O/W emulsion, which can utilize gravity as the driving force, the separation of W/O emulsion requires an additional driving source, a vacuum pump at the permeate side in this study, to force the oil across the membrane (Fig. S1c in Supporting information). However, the applied pressure should not exceed the LEP of water, otherwise the water phase would also penetrate the membrane. Therefore, the applicable pressure window lies between the oil LEP and the water LEP of each membrane. In this study, we keep the Δp (the pressure above the corresponding oil LEP) constant (10 kPa) for every membrane in the following tests.

Prior to the W/O emulsion separation tests, the basic flux for the pure transformer oil on the as-prepared membranes was measured. The pristine alumina membrane had a flux close to zero, owing to the relatively low Δp applied. The C_3/M, C_{10}/M, and C_{10}-F/M membranes had similar fluxes between 15 and 20 L m^{-2} h^{-1} bar^{-1} (Fig. S3 in Supporting information). Overall, the fluorinated silane-modified membranes delivered higher fluxes than the nonfluorinated ones. The promoting effect of the fluorinated silane modification on flux might be ascribed to the fact that the fluorinated silane could form a self-lubricate layer on the membrane surface [27], which facilitated the mass transfer of the oil molecules. Unexpectedly, the C_3-F/M membrane afforded a much higher flux relative to all the other membranes. This might be ascribed to two aspects: (1) The short carbon chain of C_3 that induced a low mass transfer resistance; and (2) the smaller roughness (less SiO_2 NPs formed by silane hydrolysis) on the surface that induced appropriate surface energy [28]. The latter was suggested to be one more decisive factor for the flux as the C_3/M and C_{10}/M delivered similar fluxes.

The W/O emulsion separation was first tested using a water-transformer oil mixture (v:v = 1:1) without Span 80. The average size of the prepared emulsion was ~2.6 μm in diameter (Fig. 3a). As observed in Fig. 3b, only the pristine membrane did not have measurable flux, similar to the result shown in Fig. S3. Furthermore, all four modified membranes showed complete water rejection, which could be attributed to the size exclusion effect. Flux decline was observed for C_3/M, C_3-F/M, and C_{10}/M membranes throughout the 2.0 h testing period, possibly due to the water droplets coalescing on the membrane surface and blocking the pores under negative pressure [29]. However, the flux of the C_{10}-F/M membrane increased at the beginning of the test and re-

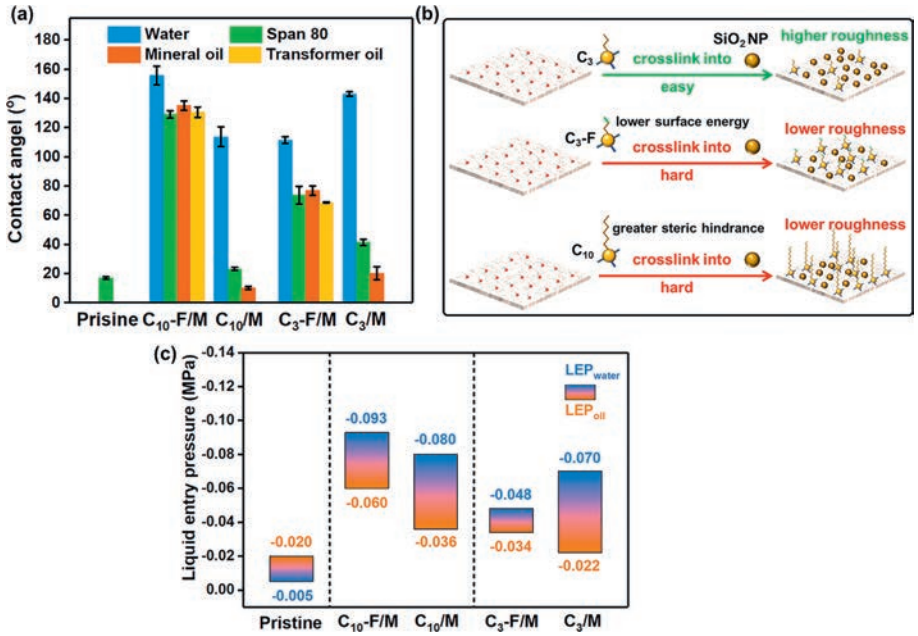

Fig. 2. (a) Contact angles of pure water, Span 80, mineral oil, and transformer oil on the as-prepared membranes. (b) The schematic diagram of silanes crosslink into silica nanoparticles. (c) Liquid entry pressures of water and transformer oil for the as-prepared membranes.

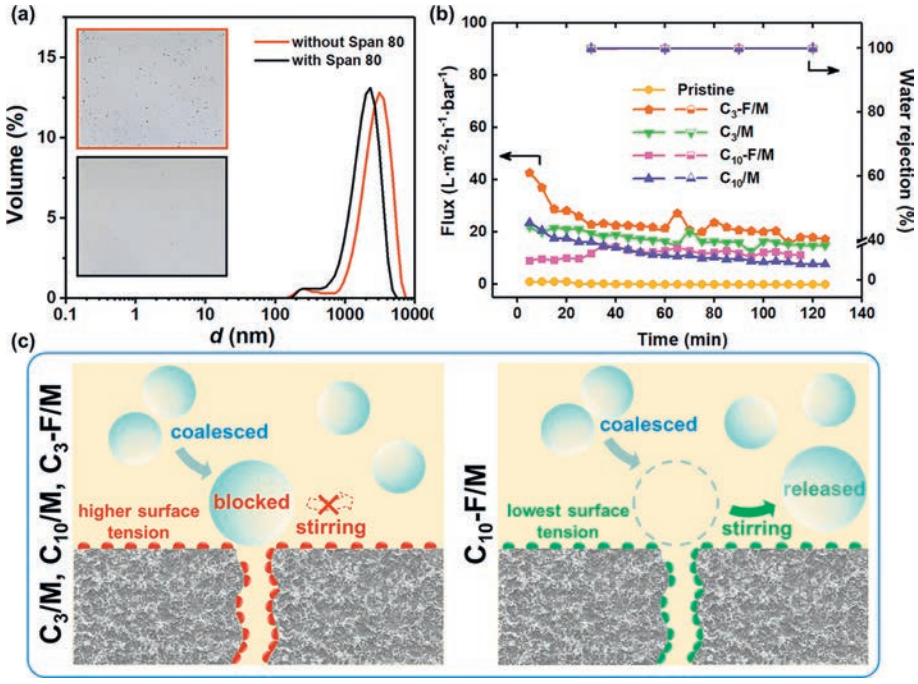

Fig. 3. (a) Size distribution of the water microdroplets from surfactant-free 1:1 W/O emulsion and surfactant-stabilized W/O emulsion. (b) Separation performance of the W/O emulsion without Span 80 using the five alumina membranes. (c) The schematic diagram of separation for surfactant-free W/O emulsion. The driving force of the separation was supplied by a vacuum pump, and the pressures for the pristine membrane and modified membranes were LEP_{water} + 0.01 MPa and LEP_{oil} + 0.01 MPa, respectively.

mained stable afterward. This phenomenon can be rationalized by the fact that the C_{10}-F/M membrane has the lowest surface tension [30,31], and thereby the water droplets could be easily coalesced and released under stirring. The process is illustrated in Fig. 3c.

The modified membranes were also used for the separation of the Span 80-stabilized W/O emulsion. The average size of the W/O emulsion was ~2.3 μm in diameter (Fig. 3a). The presence of surfactants in emulsion will usually change the interfacial property between the water droplet and oil phase, making the demulsification and separation process more challenging. As shown in Fig. 4, short-chain silane-modified membranes (C_3/M and C_3-F/M) exhibited excellent water rejection rates (96% for the C_3/M and 97% for the C_3-F/M), which were slightly better than the C_{10} (92%). All of the modified membranes exhibited reduced original flux compared with the results shown in Fig. 3, suggesting that the surfactant-stabilized emulsion was easier to accumulate and block the membrane surface. One interesting observation is that the C_{10}-F/M membrane failed to separate the emulsion at the very beginning of the test, accompanied by a dramatic flux decline. Unlike the separation of surfactant-free W/O emulsion, the pris-

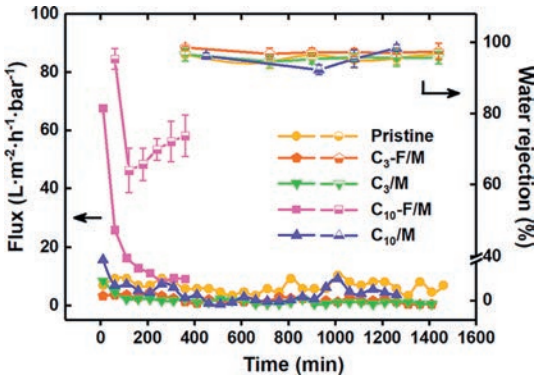

Fig. 4. Separation performance of the Span 80-stabilized W/O emulsion using the five alumina membranes. The driving force of the separation was supplied by a vacuum pump, and the pressures for the pristine membrane and modified membranes were LEP_{water} + 0.01 MPa and LEP_{oil} + 0.01 MPa, respectively.

tine membrane shows separation ability for the Span 80-stabilized W/O emulsion. For surfactant-free W/O emulsion, water droplets have a great affinity with the membrane surface, resulting in water droplets adsorbed on the surface and blocked the hole. After adding Span 80, water droplets did not come into direct contact with the membrane surface, thus, the pristine membrane could separate the emulsion. Nevertheless, all the tested membranes, including the failed C_{10}-F/M membrane, had similar and relatively stable oil fluxes during the 24 h continuous separation test, and they also show stable separation performance for another Span 80-stabilized water-in-mineral oil emulsion during five cycles (Fig. S4 in Supporting information), which indicates the high stability of these membranes.

Since the results of W/O emulsion separation with or without surfactant are substantially different, it is evident that the presence of Span 80 changed the membrane separation behavior. As shown in Fig. 3a, the droplet sizes of the W/O emulsion with and without Span 80 were similar and much larger than the membrane pore size (>2 μm *vs.* 100 nm). Therefore, the major separation mechanisms are size exclusion and the hydrophobic surface that repels the water phase, in agreement with literature reports [32]. However, the distinct behaviors observed on the pristine membrane indicate that the addition of Span 80 lowered the oil penetration threshold on the pristine membrane, which could result from the lowered liquid surface tension. Meanwhile, the full rejection of the water phase on the pristine membrane could be ascribed to the fact that the membrane surface was fully wetted by the oil phase. Therefore, the pristine membrane performed well in separating the Span 80-stabilized W/O emulsion.

Although the C_{10}-F/M membrane has the lower surface energy among the modified membranes (2.76 mN/m for C_{10}-F/M and 3.06 mN/m for C_{10}/M), it unexpectedly failed to separate the surfactant-contained W/O emulsion. The average emulsion size of the permeate was about 1 μm (Fig. S5 in Supporting information), still much larger than the pore size. This failure is unlikely due to the water droplets breaking down into smaller nano-sized droplets, as this process generates more water/oil interface and is thermodynamically highly unfavorable. Therefore, we must consider the possibility that the water droplets penetrate the membrane without size breakdown. This is also a thermodynamically unfavorable process because it would increase the droplet surface area and the surface energy. However, this process would be possible in the presence of Span 80 to lower the interfacial tension and a cross-membrane driving force to overcome the deformation energy barrier. On the other hand, C_{10}-F/M membrane modification has the lowest surface energy among the four silanes and has been reported as a "slippery" coating in many studies [33,34]. We believe that this slippery nature of the C_{10}-F coating further reduces the energy required for the water droplet deformation and enables the droplets to penetrate the membrane.

To verify the above assumption, the C_{10}-F/M and C_{10}/M membranes were selected for the further characterization of water rejection in the separation of W/O emulsion under increased operating pressure (Figs. 5a and b). When separating the surfactant-free W/O emulsion, the increased operating pressure resulted in a limited reduction in the separation performance (Fig. 5a). Their water rejection rates were still greater than 96% under a high operating pressure of −0.09 MPa. For surfactant-stabilized W/O emulsion, the water rejection of C_{10}-F/M and C_{10}/M membranes reduced as the pressure increased (Fig. 5b). The C_{10}-F/M membrane completely failed to separate Span 80-stabilized W/O emulsion under high operating pressure. When applied the same operating pressure, both the C_{10}-F/M and C_{10}/M membranes showed higher water rejections in the separation of surfactant-free W/O emulsion as compared to Span 80 stabilized W/O emulsion. This phenomenon indicates that Span 80 lower the deformation energy of water droplets, thus allowing them to enter the membrane pores more easily.

A mechanistic insight was proposed to better understand the interaction of modified membranes with water droplets under various conditions (with or without Span 80 surfactant) during the separation process (Figs. 5c and d). The interaction force between the water droplets and the C_{10}M was higher than that on the C_{10}-F/M. Consequently, the water droplets must overcome a larger resistance as they attempt to deform and permeate the C_{10}M. In other words, it is more difficult for the water droplets to deform with C_{10}M under the same operating pressure condition. Thus, C_{10}M offers better water rejection than C_{10}-F/M at elevated operating pressures. As a comparison, fluorinated long carbon chain silane-modified C_{10}-F/M membrane displays a "slippery" surface, which causes little interaction force between water droplets and C_{10}-F/M. Moreover, the combination of surfactant, the "slippery" surface, and an elevated pressure facilitates the deformation and penetration of water droplets. This phenomenon emphasizes the importance of membrane surface wettability and the interfacial interaction between the droplets and membrane pores for W/O separation. It is essential to engineer a surface with proper wettability, which could stop the water phase while allowing the transport of the oil phase.

Another issue that should be mentioned is the low oil flux of our membranes compared with the fluxes reported in the literature. There are several reasons accountable for this issue. First, the oil we used in this study was transformer oil with a much higher dynamic viscosity than those organic solvents used in the literature (such as alkane and toluene), making the mass transfer much slower. Second, the substrate membrane used in this study has a pore size of 100 nm, much smaller than those micron-sized membranes used in other studies.

The separation of W/O emulsion is still a challenging task for wastewater treatment. Our results suggest that while the membrane technology is a competitive candidate for emulsion separation, the membrane surface wettability should be carefully engineered to achieve desired separation goals. The comparison using four different silanes demonstrates that although long-chain fluorinated silane gives low surface energy to the membrane, it does not necessarily deliver the best separation performance. In our case, the C_3-F/M membrane, a short-chain and partially fluorinated silane, exhibited the best performance in terms of flux and water rejection. The continuous and cyclic emulsion separation tests also suggest that the silane-modified alumina membrane has excellent stability and separation performance. Furthermore, our observations emphasize the correlation between the surface wettability and separation mechanism, which could be extended to other emulsion systems.

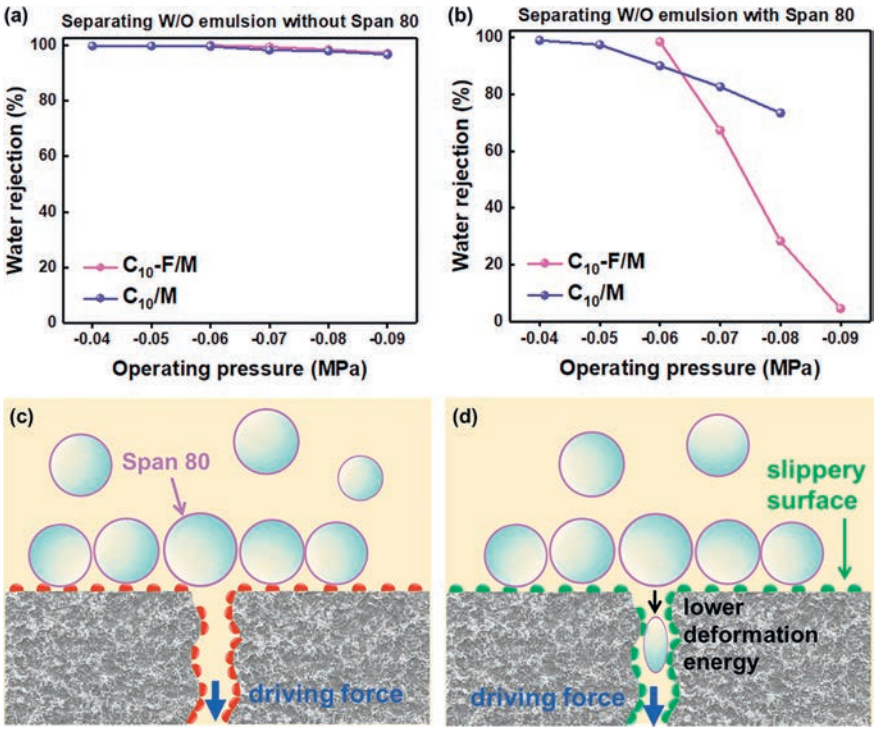

Fig. 5. Water rejection of C_{10}-F/M and C_{10}/M membranes for the separation of W/O emulsion without (a) or with (b) Span 80 under different operating pressure, mechanistic insights into interaction of the C_{10}/M (c) and C_{10}-F/M (d) modified membranes and water droplets with Span 80. The driving force of the separation was supplied by a vacuum pump, and the pressures for C_{10}/M and C_{10}-F/M were ranged from −0.04 MPa to −0.09 MPa.

Declaration of competing interest

The authors declare no conflict of interest.

Acknowledgments

This work is supported by the Guangzhou Science and Technology Plan (No. 202102020219), National Natural Science Foundation of China (No. 51908565), and High-level talent research start-up project of Chongqing Technology and Business University (No. 2356007).

Supplementary materials

Supplementary material associated with this article can be found, in the online version, at doi:10.1016/j.cclet.2023.109090.

References

[1] S. Ding, X. Han, L. Zhu, et al., Water Res. 232 (2023) 119684.
[2] T. Ni, Y. You, Z. Xie, et al., J. Membr. Sci. 653 (2022) 120543.
[3] H.J. Tanudjaja, C.A. Hejase, V.V. Tarabara, et al., Water Res. 156 (2019) 347–365.
[4] M. Wang, H.S. Tsai, C. Zhang, et al., Chin. Chem. Lett. 33 (2022) 2807–2816.
[5] D. Shi, T. Gong, R. Wang, et al., Water Res. 237 (2023) 119984.
[6] D. Jiang, C. Gao, L. Liu, et al., Sep. Purif. Technol. 295 (2022) 121317.
[7] I. Krupa, A. Mahmoud, P. Sobolciak, et al., Sep. Purif. Technol. 302 (2022) 122118.
[8] Y. Shi, Q. Zheng, L. Ding, et al., Environ. Sci. Technol. 56 (2022) 4518–4530.
[9] L. Zhu, W. Wang, P. Zhao, et al., Water Res. 226 (2022) 119209.
[10] X. Wang, K. Sun, G. Zhang, et al., Water Res. 208 (2022) 117859.
[11] X. Zhao, Y. Jiang, L. Cheng, et al., Chin. Chem. Lett. 33 (2022) 3859–3864.
[12] T. Gu, Q. Zhang, R. Shi, et al., ACS Sustain. Chem. Eng. 10 (2022) 15243–15249.
[13] Q. Guo, Y. Huang, M. Xu, et al., J. Membr. Sci. 664 (2022) 121115.
[14] Y. Hu, P. Zhao, H. Liu, et al., Chin. Chem. Lett. 34 (2023) 107931.
[15] B.J. Deka, E.J. Lee, J. Guo, et al., Environ. Sci. Technol. 53 (2019) 4948–4958.
[16] S. Ruidas, A. Das, S. Kumar, et al., Angew. Chem. Int. Ed. 61 (2022) e202210507.
[17] W. Zhang, J. Gao, Y. Deng, et al., Adv. Funct. Mater. 31 (2021) 2101068.
[18] J. Li, S. Huang, L. Zhang, et al., Sep. Purif. Technol. 313 (2023) 123480.
[19] J. Zhang, L. Zhu, S. Zhao, et al., Colloids Surf. A 625 (2021) 126843.
[20] A. Wang, T. Cao, H. Tang, et al., Colloids Surf. B 47 (2006) 57–63.
[21] C. Boo, J. Lee, M. Elimelech, Environ. Sci. Technol. 50 (2016) 8112–8119.
[22] Y.X. Huang, Z. Wang, J. Jin, S. Lin, Environ. Sci. Technol. 51 (2017) 13304–13310.
[23] Y.X. Huang, D.Q. Liang, C.H. Luo, et al., J. Membr. Sci. 637 (2021) 119673.
[24] T. Horseman, Y. Yin, K.S.S. Christie, et al., ACS ES&T Engg. 1 (2021) 117–140.
[25] A.C.M. Franken, J.A.M. Nolten, M.H.V. Mulder, et al., J. Membr. Sci. 33 (1987) 315–328.
[26] M.C. García-Payo, M.A. Izquierdo-Gil, C. Fernández-Pineda, J. Colloid Interface Sci. 230 (2000) 420–431.
[27] B. Li, K. Li, Appl. Surf. Sci. 598 (2022) 153782.
[28] S. Peppou-Chapman, J.K. Hong, A. Waterhouse, C. Neto, Chem. Soc. Rev. 49 (2020) 3688–3715.
[29] Z. Gao, X. Gu, C. Liu, et al., J. Membr. Sci. 660 (2022) 120842.
[30] X. Hu, Y. Xu, J. Wang, et al., Chem. Eng. J. 451 (2023) 139031.
[31] J. Hu, H. Li, Z. Liu, G. Jiang, Surf. Coat. Tech. 425 (2021) 127646.
[32] T.M. Schutzius, C. Walker, T. Maitra, et al., Langmuir 33 (2017) 4250–4259.
[33] L. Liu, Z. Xiao, Y. Liu, et al., Desalination 499 (2021) 114864.
[34] X. Zhao, B. Khatir, K. Mirshahidi, et al., ACS Nano 15 (2021) 13559–13567.